

# ROLE OF (NA, BI) EXCESS MOL% ON DIELECTRIC, FERROELECTRIC AND PIEZOELECTRIC PROPERTIES OF $\text{Na}_{0.5}\text{Bi}_{0.5}\text{TiO}_3$ CERAMIC

K. Parmar and N.S. Negi

Department of Physics, Himachal Pradesh University, Shimla 171005, India

## ABSTRACT

Lead free ceramics based on  $(\text{Na}_{0.5}\text{Bi}_{0.5})_{1+x}\text{TiO}_3$  with different excess mol% of Na/Bi volatiles were synthesised by sol-gel method. The x-ray diffraction and Raman spectra analyses reveal that excess mol% of Na/Bi volatiles cause local disorders without disturbing the whole perovskite structural symmetry of  $(\text{Na}_{0.5}\text{Bi}_{0.5})_{1+x}\text{TiO}_3$  ceramics. The surface morphology of samples is improved in terms of homogeneity and density with excess to that of without excess of Na/Bi volatiles. The excess of Na/Bi at  $x = 0.02$  leads to stoichiometric composition with compact crystal growth and improved properties such as DC resistivity ( $\rho_{DC} = 4.9 \times 10^{11}$  ohm-cm), dielectric, ferroelectric ( $P_r = 20.5 \mu\text{C}/\text{cm}^2$ ) and piezoelectric ( $d_{33} = 97 \text{pC}/\text{N}$ ) properties. The compositional fluctuations induced by Bi loss and higher Na/Bi excess concentration for  $(\text{Na}_{0.5}\text{Bi}_{0.5})_{1+x}\text{TiO}_3$  samples with  $x = 0$  and  $x > 0.02$  are observed to affect ferroelectric and piezoelectric properties.

**KEYWORDS:** Lead free ceramic; Sol-gel process; Raman spectra; Dielectric properties; Ferroelectric properties

## I. INTRODUCTION

Lead based perovskite oxides posing excellent ferroelectric properties constitute important class of materials due to their tremendous use in various applications like sensor, actuators, transducers and micro-electro-mechanical devices etc. [1, 2]. However, formation of toxic PbO during synthesis has mostly restricted their commercial use in order to avoid harmful effects on environment [3, 4]. Sodium bismuth titanate ( $\text{Na}_{0.5}\text{Bi}_{0.5}\text{TiO}_3$ ) based solid solutions having morphotropic phase boundary (MPB) analogous to Pb based materials (PZT) are recognised as most promising lead free ferroelectric materials and may replace Pb based materials up to some extent [5-7]. Moreover, pure Sodium Bismuth Titanate has some distinctive issues which are capturing much research attention recently such as ambiguity over its structure at room temperature, controversies on temperature dependent phase transitions and high leakage current problems [8, 9]. Earlier studies revealed that NBT system exhibits rhombohedral structure (R3c) at room temperature [10-15]. Also, recently Rao *et al.* [16] reported first principle study along with electric field dependent electron, neutron and XRD studies and suggested that global rhombohedral (R3C) phase is more stable for NBT system. While, some research groups reported monoclinic (Cc) order of NBT system at room temperature [17, 18]. Complexity of NBT structure depends on in-phase/out-of-phase octahedral tilting due to random distributions and different displacements of Bi/Na cations [5, 19, 20]. The A-site composition of  $(\text{Na}_{0.5}\text{Bi}_{0.5})\text{TiO}_3$  system may be varied intentionally by taking non-stoichiometric proportion of Na/Bi volatiles or unintentionally due to high temperature loss of volatile elements during synthesis. The non-stoichiometric order at A site of perovskite structure having volatile elements has an effect on growth and densification of materials such as (Na,Bi) in NBT system analogues to Pb in Pb based materials [21]. It is reported earlier that A-site cations deficiency degrades the densification to some extent, in contrast, the A-site cation excess advances the sintering [22]. Either Bi excess or Na deficiency has been reported to induce same impact in  $\text{Na}_{0.5}\text{Bi}_{0.5}\text{TiO}_3$  matrix such as decrease in grain

size assist crystal densification which result in enhanced piezoelectric coefficient ( $d_{33}$ ) and lower depolarization temperature ( $T_d$ )[23]. In most, Na and Bi non-stoichiometry have been independently studied in NBT based systems and accounted for improved dielectric, ferroelectric and piezoelectric properties [24, 25]. Hence keeping in view the crucial role of stoichiometry on properties of NBT based system; here we present the impact of both Na and Bi excess mol% on structural, dielectric, ferroelectric and piezoelectric properties of pure  $\text{Na}_{0.5}\text{Bi}_{0.5}\text{TiO}_3$  lead free system.

## II. EXPERIMENTAL DETAILS

Lead free  $(\text{Na}_{0.5}\text{Bi}_{0.5})_{1-x}\text{TiO}_3$  ceramics were prepared by sol gel method with different compositions having  $x=0, 0.02, 0.05$  and  $0.1$  which correspond to Na/Bi 0, 1, 2.5 and 5 excess mol%. The samples are hereafter named as NBT0, NBT1, NBT2.5 and NBT5 respectively. Pure powders (Analytical grade, Merck) of sodium nitrate ( $\text{NaNO}_3$ ) and bismuth nitrate ( $\text{Bi}(\text{NO}_3)_3 \cdot 5\text{H}_2\text{O}$ ) were weighed according to designed chemical formula. These powders were dissolved in acetic acid with uniform stirring. Tetran-butyl titanate ( $\text{Ti}(\text{OC}_4\text{H}_9)_4$ ) was mixed with acetyl acetone and 2-propanol in weight ratio of 1:3:5 to avoid its hydrolysis. The resulting stable solution of Ti was added drop wise to the solution of nitrates to get Na-Bi-Ti complex solution. The complex solution was stirred at  $65^\circ\text{C}$  temperature for 2 h and then mixed with the aqueous solution of citric acid taken in 1.2:1 weight ratios to nitrates. The resulting solution was dried at  $80^\circ\text{C}$  temperature to form gel which subsequently transformed into a powder. Heat treatment was given in steps, at  $350^\circ\text{C}$  for 0.5 h to remove hydrocarbons, pre-calcination at  $650^\circ\text{C}$  for 3 h and final calcination at  $850^\circ\text{C}$  for 2 h to achieve crystallisation. The calcined powders were uniformly mixed with 3% aqueous solution of PVA used as binder and pelletized in pellets of diameter 9mm and thickness  $\sim 0.8$  to 1.2 mm using a hydraulic press and sintered at  $1050^\circ\text{C}$  for 2 h. Samples sintered at  $1050^\circ\text{C}$  were used for structural and electrical analysis. Silver (Ag) paste is coated on both sides of pellets and dried at  $300^\circ\text{C}$  temperature for 0.5 h to make ohmic contacts for electrical measurements.

Room temperature x-ray diffraction patterns of the samples were carried out by Panalytical's X'Pert Pro x-ray diffractometer using  $\text{CuK}\alpha$  radiation. Surface morphology and chemical element compositions of samples were determined using scanning electron microscopy (SEM) (Quanta 250, FEI make, Model No. D9393) equipped with an energy dispersive X-ray(EDS) detector. The Raman spectra of samples were carried out using iHR550 imaging Spectrometer(Make: JY HORIBA).The dielectric properties were measured by using an impedance analyzer (Wayne Kerr 6500B). The ferroelectric properties were studied by using P-E loop tracer(modified Sawyer-Tower circuit)of Marine India Ltd. at frequency of 50 Hz. For piezoelectric properties, pellets were poled electrically at 4 kV/mm in silicon oil bath at  $85^\circ\text{C}$  temperature for 2 h and piezoelectric coefficient ( $d_{33}$ ) was measured by Piezo-Meter(Take Control, PM-35,UK).

## III. RESULTS AND DISCUSSION

### X-ray Diffraction

Fig. 1(a) shows x-ray diffraction patterns of  $(\text{Na}_{0.5}\text{Bi}_{0.5})_{1+x}\text{TiO}_3$  ceramic with different Na/Bi mol% excess compositions. It can be seen that all NBT ceramics exhibit typical diffraction peaks of  $\text{ABO}_3$  perovskite structure and no other secondary phase is observed on increasing Na/Bi excess mol% up to 5 mol% at  $1050^\circ\text{C}$  sintering temperature. The XRD patterns of samples shown in Fig. 1 are in good agreement with previously reported structural analysis of non-stoichiometric  $\text{Na}_{0.5}\text{Bi}_{0.5}\text{TiO}_3$  ceramics [13, 26]. Rietveld refinement (FULLPROF software package-version 2000) of the room temperature X-ray diffraction data reveals rhombohedral hexagonal symmetry with the  $R3c$  space group for all samples as shown in Fig. 1(b). The lattice and refinement parameters obtained from Rietveld fitting are given in Table 1. No significant structural change has been observed in XRD patterns of NBT ceramics with varying excess mol% of Na and Bi. However, the close view of (024) diffraction peak over  $2\theta$  range of  $46.5^\circ$  to  $47.5^\circ$  as shown in inset of Fig. 1(a) depicts that the (024) peak first shifts towards the lower  $2\theta$  side for 1 mol% excess of Na and Bi (NBT1) followed by gradual shifting of the peak towards the higher peak  $2\theta$  value for NBT ceramic with 2.5 mol% excess of Na and Bi (NBT2.5). With further increasing of Na and Bi excess mol% to 5mol% (NBT5) the peak slightly shifts towards the lower  $2\theta$  value with significant reduction in the peak intensity. Usually a systematic

shift in XRD reflection lines has been reported for either excess of Bi or deficiency of Na in NBT ceramics [23, 27].

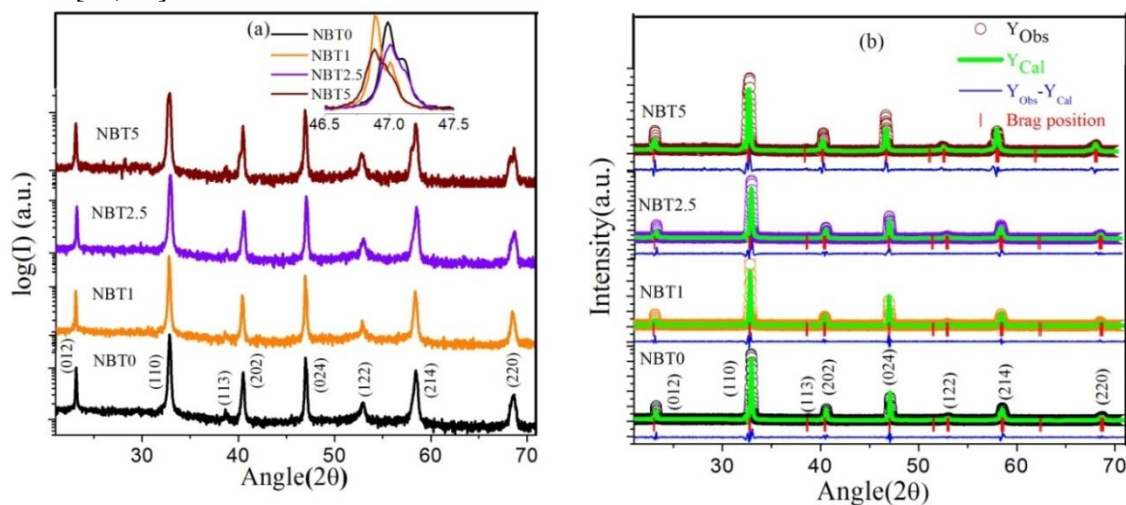


Fig. 1. (a)XRD patterns (b) Rietveld analysis of XRD patterns for  $(\text{Na}_{0.5}\text{Bi}_{0.5})_{1+x}\text{TiO}_3$  ceramics

Table 1. Rietveld refinement results (lattice parameters, cell volume), relative density ( $\rho_r$ ) and dc resistivity( $\rho_{DC}$ ) for  $(\text{Na}_{0.5}\text{Bi}_{0.5})_{1+x}\text{TiO}_3$  ceramics

Parameters(units)	NBT0	NBT1	NBT2.5	NBT5
a=b (Å)	5.4711	5.4726	5.4698	5.4732
c (Å)	13.3720	13.3845	13.3639	13.3780
Cell volume (in Å <sup>3</sup> )	346.6	347.2	346.3	347.1
$R_p, R_{wp}, \chi^2$	11.1, 16.3, 3.75	10.8, 16.0, 2.94	13.1, 18.2, 3.81	13.9, 19, 4.08
$\rho_r$ (%)	86	97	90	94
$\rho_{DC}$ (ohm-cm)	$4.6 \times 10^{11}$	$4.9 \times 10^{11}$	$3.8 \times 10^9$	$1.2 \times 10^9$

However, we have not observed such behavior in our Na and Bi excess NBT samples which indicates that excess of both Na and Bi plays a complex role in NBT system. Comparative intense and sharp XRD peak of NBT1 sample reveals uniform and large crystallites attributing that 1mol% excess of Na/Bi compensates the evaporation of volatiles and leads to growth of stoichiometric  $\text{Na}_{0.5}\text{Bi}_{0.5}\text{TiO}_3$  crystals which is also supported by lattice parameters and relative density measurements, given in Table 1. However, Bi loss in NBT0 sample and extravagant Na/Bi excess mol% in NBT2.5-NBT5 samples may contribute to compositional fluctuations and lattice deformation leading to distort and small intense XRD peak. The detail of density measurements is given in our previous work reported elsewhere [28].The relative density ( $\rho_r$ ) of NBT sample with 1 mol% excess of Na/Bi is observed significantly higher than other samples(Table 1) which may be attributed to the compact crystal growth.

### Scanning Electron Microscopy

Surface morphology of the samples are studied by scanning electron microscope (SEM) and shown in Fig. 2. The SEM micrographs represent polycrystalline nature of all samples.The average grain sizes of NBT0, NBT1, NBT2.5 and NBT5 ceramics are estimated using ImageJ software and are  $\sim 1.13\mu\text{m}$ ,  $\sim 1.26\mu\text{m}$ ,  $\sim 1.18\mu\text{m}$  and  $\sim 1.15\mu\text{m}$  respectively. Average grain size increases up to NBT1( $x=0.02$ ) and small variation is observed for further addition of Na/Bi volatiles. It can be clearly seen in SEM micrographs that NBT1 sample having 1 mol% excess of Na/Bi exhibits dense crystal growth with better grain connectivity as compared to other samples that is in good agreement with density evaluation under Rietveld refinement of XRD patterns discussed previously.

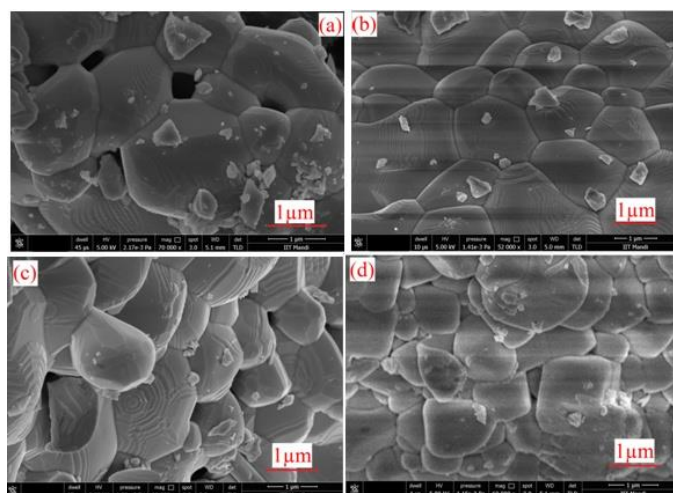


**Fig. 2.** SEM images of  $(\text{Na}_{0.5}\text{Bi}_{0.5})_{1+x}\text{TiO}_3$  ceramics where (a) NBT0, (b) NBT1, (c) NBT2.5 and (d) NBT5

The qualitative and quantitative compositional analyses of the elements present in  $(\text{Na}_{0.5}\text{Bi}_{0.5})_{1+x}\text{TiO}_3$ ,  $x = 0, 0.02, 0.05$  and  $0.1$  samples sintered at  $1050^\circ\text{C}$  temperature have been studied by Energy Dispersive X-ray spectrometer (EDS) attached to the SEM instrument and the corresponding EDS spectra are shown in Fig. 3. The results indicate that constituent elements are present in the samples in expected weight and atomic percentages. It is clear that the synthesized samples do not exhibit any other impurities apart from the constitutional elements of the  $(\text{Na}_{0.5}\text{Bi}_{0.5})_{1+x}\text{TiO}_3$  system. The EDS spectra have been measured 2 to 3 times by changing selective area of each sample to carry out a reliable quantitative analysis. The most probable trend of atomic and weight compositions in various NBT ceramics is given in Table 2. The values observed for these samples indicate that NBT1 ceramic with 1 mol% excess of Na/Bi volatiles seems more stoichiometric as the observed atomic% of all elements is close to theoretical atomic% of  $\text{Na}_{0.5}\text{Bi}_{0.5}\text{TiO}_3$  and Bi/Na ratio approaches to  $\sim 1$  (i.e. 0.988) while comparing with other remaining samples having Na and Bi 0, 2.5 and 5mol% excess corresponding to  $x=0, 0.05$  and  $0.1$ . It is observed that Bi loss is more pronounced in  $\text{Na}_{0.5}\text{Bi}_{0.5}\text{TiO}_3$  sample without Na/Bi excess, whereas excess of alkali metal (Na) concentration can be seen in NBT ceramics with 2.5 and 5mol% excess of Na and Bi elements.

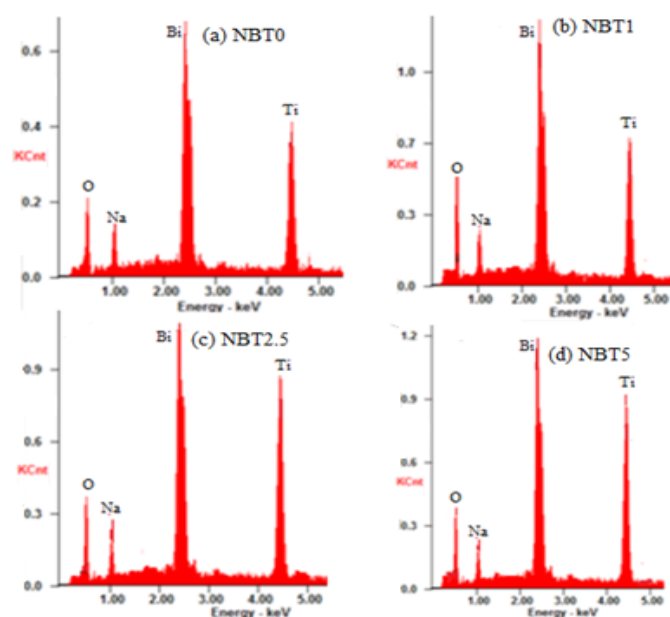


**Fig. 3.** EDS spectra of  $(\text{Na}_{0.5}\text{Bi}_{0.5})_{1+x}\text{TiO}_3$  ceramics with (a) 0, (b) 1, (c) 2.5 and (d) 5 mol% excess of Na and Bi

**Table 2.** Atomic% and weight% deduced from EDS measurements for  $(\text{Na}_{0.5}\text{Bi}_{0.5})_{1+x}\text{TiO}_3$  ceramics sintered at  $1050^\circ\text{C}$  for 2 h

Elements	Atomic%				Weight%			
	NBT0	NBT1	NBT2.5	NBT5	NBT0	NBT1	NBT2.5	NBT5
Bi	9.26	10.08	10.59	11.08	48.12	49.82	49.78	50.04
Na	10.19	10.20	12.11	14.15	5.86	5.98	6.42	6.94
Ti	20.61	19.99	19.80	20.13	24.96	23.26	22.35	23.02
O	59.94	59.73	57.50	54.64	21.02	20.94	21.45	20
Bi/Na	0.909	0.988	0.874	0.783	8.21	8.33	7.75	7.21

Hirumaet al.[29] reported that small deviation in A-site cations (Na/Bi) stoichiometry drastically change the room temperature DC resistivity of NBT system by 3 orders of magnitude and influence the dielectric, ferroelectric and piezoelectric properties. In particular, Bi excess or Na deficiency in the starting  $\text{Na}_{0.5}\text{Bi}_{0.5}\text{TiO}_3$  composition enhance the DC resistivity and piezoelectric coefficient ( $d_{33}$ ) but lowers the depolarization temperature ( $T_d$ ). In contrast, DC resistivity and  $d_{33}$  decrease and  $T_d$  enhances with Na excess or Bi deficient in  $\text{Na}_{0.5}\text{Bi}_{0.5}\text{TiO}_3$  ceramic[23, 27, 30, 31]. In present work, room temperature DC resistivity of samples has been measured by using two probe method and values are given in Table1. An abrupt decrease in order from  $10^{11}$  to  $10^9 \Omega\text{-cm}$  is observed as Na/Bi excess mol% raises from 1mol% (NBT1) to 5mol% (NBT5) signifying the presence of highly conductive alkali (Na) ions at A-site which further support the EDS analysis. Also, the large value of DC resistivity of NBT1 ( $\rho_{DC} = 4.9 \times 10^{11} \text{ ohm-cm}$ ) confirms that 1mol% excess of Na/Bi volatiles leads to formation of stoichiometric composition with comparative small defects or vacancies.

#### Compositional Dependent Raman Spectroscopy

The short length scale ordering of perovskite structural phase of  $(\text{Na}_{0.5}\text{Bi}_{0.5})_{1+x}\text{TiO}_3$  samples have been analysed using Raman spectra in the range of  $100\text{-}900 \text{ cm}^{-1}$  measured at room temperature and are shown in Fig. 4.

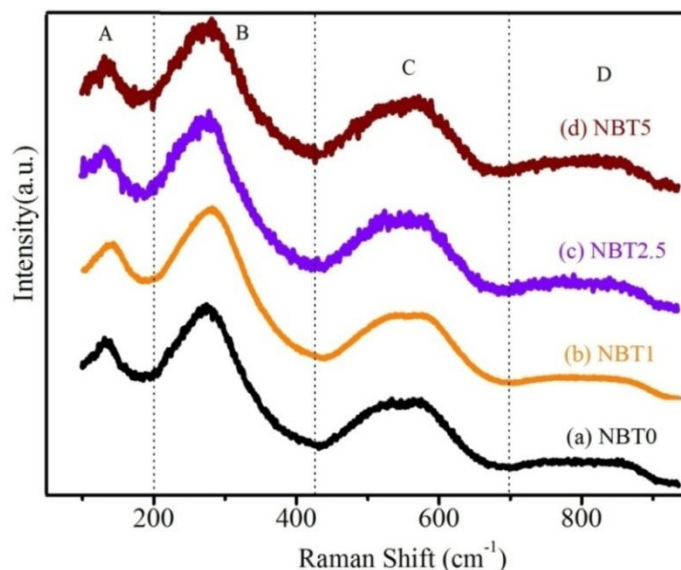


**Fig. 4.** Raman spectra of non-stoichiometric  $(\text{Na}_{0.5}\text{Bi}_{0.5})_{1+x}\text{TiO}_3$  ceramics with (a) 0, (b) 1, (c) 2.5 and (d) 5 mol% excess of Na and Bi

It was reported that in NBT ceramics having  $R3c$  crystal symmetry, the A-site disorder affects optically active modes by reducing from 18 ( $9A_1+9E$ ) to 13 ( $4A_1+9E$ ) optical modes [32], where  $A_1$  and  $E$  are both Raman/IR active modes. In Fig. 4, the spectra can be grouped into four frequency regions: (A)  $100\text{-}200 \text{ cm}^{-1}$ , (B)  $200\text{-}450 \text{ cm}^{-1}$ , (C)  $450\text{-}700 \text{ cm}^{-1}$  and (D)  $700\text{-}900 \text{ cm}^{-1}$ . According to Kreisel *et al.*[33], the vibration mode in region A is associated with Bi/Na-O vibrations, the broad and highly intense band in region B is assigned to Ti-O vibrations, the modes in region C are associated with  $\text{TiO}_6$  octahedral vibrations and finally region D in the high frequency range is mainly due to the

vibrations involving oxygen displacements. It can be seen from Raman spectra that all the major bands which are characteristics of vibrational modes in pure NBT system exist in all samples and observed Raman spectrum for NBT0 is in agreement with the previously reported results [34]. The peak position of Raman active mode can be specified by fitting the measured spectra and decomposing the fitted curves into separate Lorentzian components. The individual deconvoluted curves and fitted spectra are shown in Fig. 5. The mode frequencies has been assigned according to irreducible representation  $4A_1+9E$  used to describe the Raman active modes of rhombohedral R3c NBT ceramic [35] and are summarized Table 3. The spectra provide 6 optical modes which is less than that predicted 13 optical modes. The reduced experimental modes could be due to merging of closely spaced modes, thermal broadening and degeneracy of certain modes. One can notice that at 5 mol% Na and Bi excess in NBT5 ceramic, the spectra broaden and the intensities are observed to reduce. In addition shift in the phonon modes are observed in NBT ceramics. The A, B and C modes are first shifted to the higher frequency for 1mol% Na and Bi excess NBT1 ceramic. However, for 2.5mol% Na and Bi excess sample, the modes shift to the lower frequency side. Further, with 5 mol% Na and Bi excess in NBT5 ceramics, shift in the phonon modes towards higher frequency is observed. In other words, no systematic variation in Raman mode shift with Na and Bi excess mol% is observed.

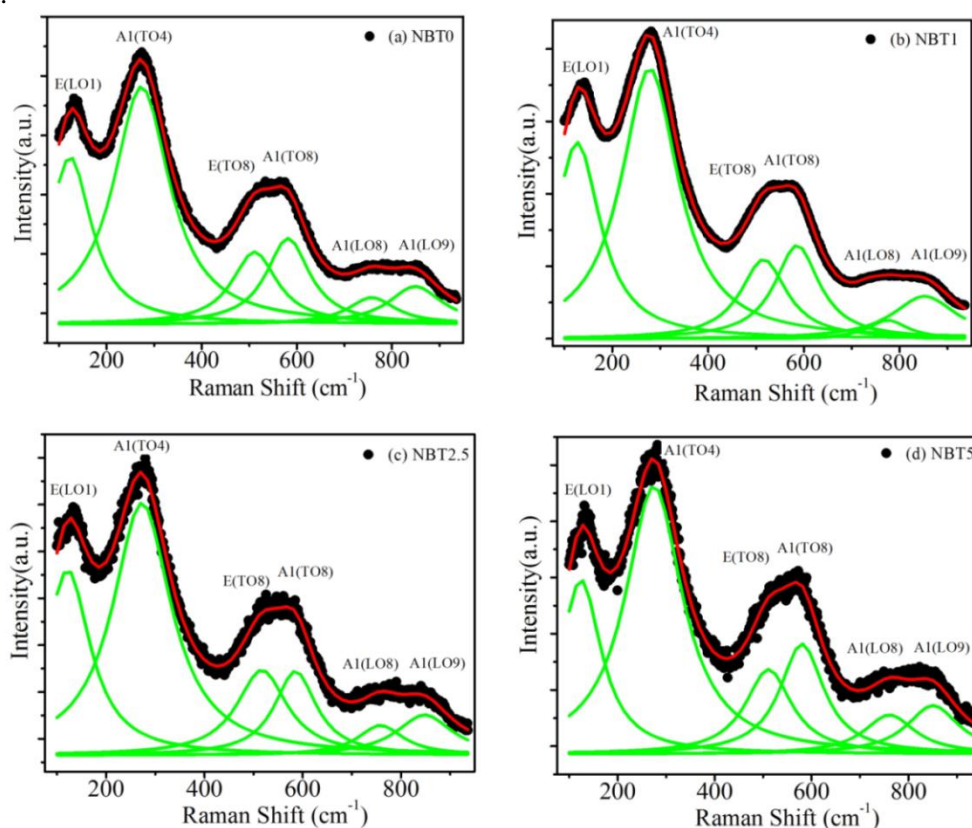


Fig. 5. Lorentz deconvoluted Raman spectra of non-stoichiometric  $(\text{Na}_{0.5}\text{Bi}_{0.5})_{1+x}\text{TiO}_3$  ceramics

Table 3. Raman bands for various  $(\text{Na}_{0.5}\text{Bi}_{0.5})_{1+x}\text{TiO}_3$  ceramics

Sample	Raman Band					
	E(LO1)	A1(TO4)	E(TO8)	A1(TO8)	A1(LO8)	A1(LO9)
NBT0	123	273	511	581	757	849
NBT1	126	278	515	586	755	849
NBT2.5	121	272	516	585	761	850
NBT5	124	274	511	580	760	850

Also, no significant shift in D modes is observed which suppresses the formation of oxygen vacancies. However, intensity variation and shifting of vibrational modes may correspond to disorderness introduced in crystal lattice with excess of Na/Bi mol%. The polycrystalline nature of the samples and random occupancy of cations of different masses at A-site ( $\text{Na}^{1+}$ ,  $\text{Bi}^{3+}$ ) may lead to broad Raman bands for all samples[36]. Similar Raman bands are observed for all samples which suggest Na/Bi excess mol% induces no structural phase change. Following Niranjana *et al.*[37], we observe three transverse modes which contribute to static dielectric tensor by providing large oscillator strength parallel:  $A_1$  (TO4),  $A_1$ (TO8) and perpendicular: E(TO8) to polar axis. These transverse modes are seem to more intense and symmetric for  $\text{Na}_{0.51}\text{Bi}_{0.51}\text{TiO}_3$ (NBT1) sample than other samples. Moreover, comparatively low intensity of vibrational mode corresponding to O shifting  $A_1$ (TO8) at  $\sim 755 \text{ cm}^{-1}$  signifies less oxygen vacancies for NBT1 sample which further supports high value of relative density and DC resistivity for this sample.

**Dielectric Studies**

Figs. 6 (a) to (d) represent the temperature dependent dielectric properties at different frequencies 1 kHz to 1 MHz measured for  $(\text{Na}_{0.5}\text{Bi}_{0.5})_{1+x}\text{TiO}_3$  ceramics.

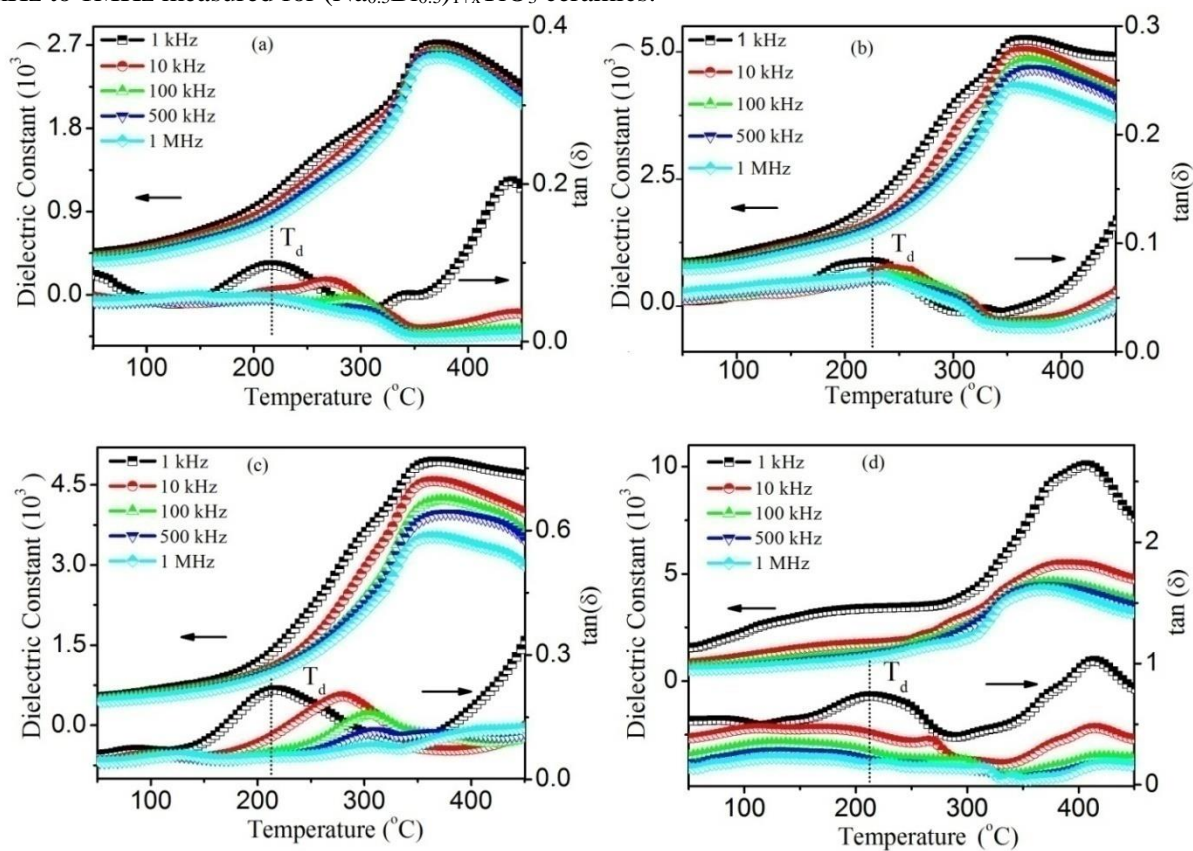


**Fig. 6.** Variation of dielectric parameters with temperature at various frequencies of  $(\text{Na}_{0.5}\text{Bi}_{0.5})_{1+x}\text{TiO}_3$  ceramics with Na/Bi excess mol% (a) 0, (b) 1, (c) 2.5 and (d) 5

**Table 4.** Depolarization temperature ( $T_d$ ) and maximum dielectric constant ( $\epsilon_m$ ) temperature ( $T_m$ ) at different frequencies of  $(\text{Na}_{0.5}\text{Bi}_{0.5})_{1+x}\text{TiO}_3$  ceramics

Sample	1 kHz			10 kHz			100 kHz			500 kHz			1 MHz		
	$T_m$ (°C)	$\epsilon_m$	$T_d$ (°C)												
NBT0	371	2708	218	371	2645	257	371	2610	280	371	2600	296	371	2564	299
NBT1	369	5237	224	365	5018	240	373	4827	262	373	4670	266	360	4306	252
NBT2.5	368	4942	210	360	4570	271	376	4208	305	373	3970	310	364	3524	312
NBT5	406	10068	220	389	5442	265	373	4586	298	369	4436	315	369	4277	320

In general, NBT system exhibits two dielectric anomalies known as depolarization temperature ( $T_d$ ) at which remnant polarization decays steeply and maximum temperature ( $T_m$ ) at which dielectric constant attains maximum value [38]. The depolarization temperature ( $T_d$ ) may involve phase transformation from field induced ferroelectric to relaxor phase or from one polar phase to another phase of different symmetry and is very crucial as it restricts high temperature piezoelectric application of NBT system.  $T_d$  is usually related to lattice distortion [39], cation vacancies [40] or oxygen vacancies [20] for NBT based ceramics. In previous reported papers, non-stoichiometry of Na or Bi in NBT system creates vacancies at A-site which produces defect field, breaks the long range ferroelectric order and results in decrease of  $T_d$  [7, 23, 27]. The values of  $T_d$ ,  $T_m$  and maximum dielectric constant ( $\epsilon'_m$ ) at  $T_m$  of all the samples at different frequencies are summarized in Table 4. In present study,  $T_d$  is determined at a temperature when  $\tan \delta$  reaches the first peak as reported in earlier works [41, 42]. The dielectric peaks at  $T_m$  for the NBT ceramics are broad suggesting that the phase transition at  $T_m$  is diffusive in nature. No variation in  $T_m$  is observed for NBT0 ceramic as a function of frequency. However, the  $\tan \delta$  peaks at  $T_d$  exhibit strong frequency dependence representing relaxor phase transition at  $T_d$ . It is observed that the  $T_m$  shifts slightly towards the lower temperatures with increasing frequencies for excess Na/Bi added NBT ceramics. Comparative high value of  $T_d$  (~224°C at 1 kHz) and small deviation on increasing frequency from 1kHz to 1MHz for NBT1 sample than other samples suggest stable ferroelectric order for this sample.

The cationic ( $\text{Na}^{1+}$ ,  $\text{Bi}^{3+}$ ) disorder at A-site is responsible for diffusive transition behavior of NBT system [43]. Also, change in diffuseness is observed with increase in Na/Bi excess mol% addition. In normal ferroelectrics, the Curie Weiss law is followed and defined as

$$\frac{1}{\epsilon'} = \frac{T - T_0}{C} \quad (T > T_0) \quad (1.1)$$

Where, C is the Curie Weiss constant describing the behavior of ferroelectric transition and  $T_0$  is the Curie Weiss temperature. In order to have detail understanding of phase transition in  $(\text{Na}_{0.5}\text{Bi}_{0.5})_{1+x}\text{TiO}_3$  ceramics, inverse dielectric constant is plotted as a function of temperature using above Curie-Weiss eq. (1.1) at frequency 100 kHz. The Curie-Weiss plots between  $\frac{1}{\epsilon'}$  and temperature exhibited straight lines with slope  $1/C$  and intercepts at x-axis taken as  $T_0$  values and are shown in Fig. 7.

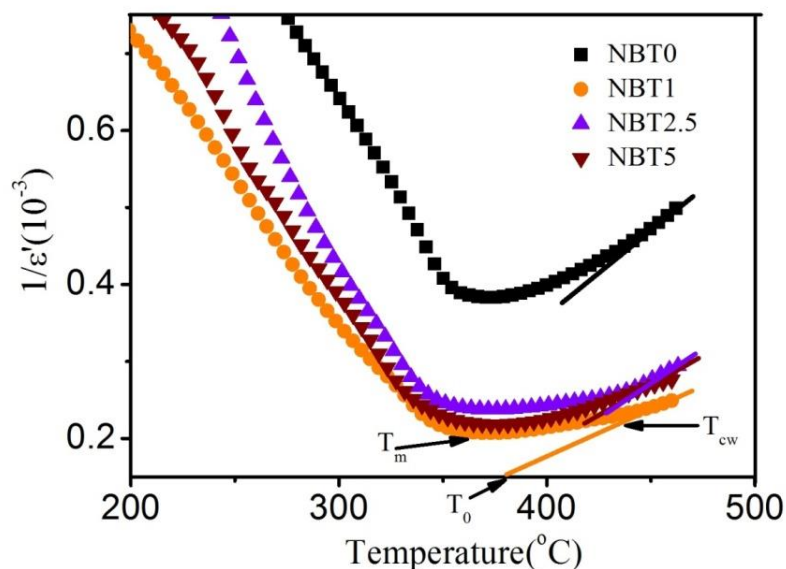


Fig. 7. Inverse dielectric constant plots as a function of temperature at 100 kHz for  $(\text{Na}_{0.5}\text{Bi}_{0.5})_{1+x}\text{TiO}_3$  ceramics

**Table 5.** The Curie-Weiss temperature ( $T_0$ ), the temperature at which  $\epsilon'$  starts to follow Curie-Weiss law ( $T_{CW}$ ), maximum dielectric constant temperature ( $T_m$ ) and deviation temperature ( $\Delta T_m$ ) for  $(\text{Na}_{0.5}\text{Bi}_{0.5})_{1+x}\text{TiO}_3$  ceramics

Sample	$T_0$ (°C)	$T_{CW}$ (°C)	$T_m$ (°C)	$\Delta T_m$ (°C)
NBT0	376	428	371	57
NBT1	381	435	373	62
NBT2.5	385	434	376	58
NBT5	380	441	373	68

The extracted parameters after fitting of eq. (1.1) are listed in Table 5. It is noticed that dielectric constant does not obey Curie-Weiss law above Curie temperature and the deviation defined by

$$\Delta T_m = T_{CW} - T_m \quad (1.2)$$

Where,  $T_{CW}$  represents the temperature from which the inverse dielectric curve follows the Curie-Weiss law.  $T_m$  is the maximum dielectric constant temperature. According to Landau's theory of phase transition, a first order transition occurs when  $T_C > T_0$  and a second order phase transition appears if  $T_C = T_0$ . In the present investigation  $T_C$  or  $T_m$  is observed close to  $T_0$  rather  $T_0$  appears slightly above  $T_m$ . Therefore, the transition is of second order. In order to quantify the diffuseness, modified form of Curie-Weiss equation suggested by Uchino and Nomura is used [44]

$$\frac{1}{\epsilon'} - \frac{1}{\epsilon'_m} = \frac{(T - T_m)^\gamma}{C} \quad 1 \leq \gamma \leq 2 \quad (1.3)$$

Where,  $\gamma$  is the degree of diffuseness with limiting values 1 and 2 for the characteristics of normal and complex diffuse phase transition respectively.  $C$  is the Curie like constant and  $\epsilon'_m$  is the maximum value of dielectric constant.

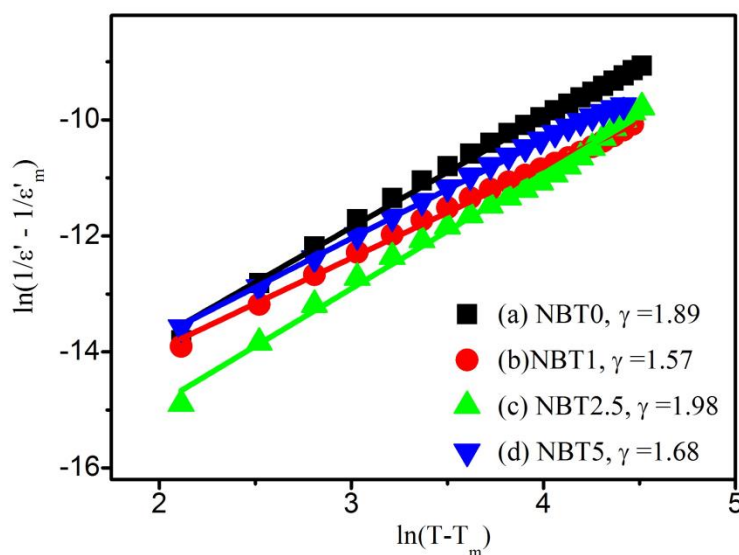


**Fig. 8.** Variation of  $\ln(1/\epsilon' - 1/\epsilon'_m)$  as a function of  $\ln(T - T_m)$  for  $(\text{Na}_{0.5}\text{Bi}_{0.5})_{1+x}\text{TiO}_3$  ceramics with Na/Bi excess mol%; (a) 0, (b) 1, (c) 2.5 and (d) 5 sintered at 1050°C temperature

The diffuseness in phase transition can be evaluated by using modified Curie –Weiss relation from the  $\epsilon'$  vs. temperature data at 100 kHz for  $(\text{Na}_{0.5}\text{Bi}_{0.5})_{1+x}\text{TiO}_3$  ceramics sintered at 1050°C, the curves between  $\ln(\frac{1}{\epsilon'} - \frac{1}{\epsilon'_m})$  vs.  $\ln(T - T_m)$  are plotted for all ceramics and shown in Fig. 8. The  $\gamma$  values observed from Curie-Weiss fitting are listed in Fig. 8. The  $\gamma$  values range from 1.57 to 1.98 suggesting diffusive behaviour and higher disorder in non-stoichiometric  $(\text{Na}_{0.5}\text{Bi}_{0.5})_{1+x}\text{TiO}_3$  ceramics.

### Ferroelectric and Piezoelectric Properties

The room temperature Polarization vs electric field (P-E) hysteresis loops of all samples are shown in Fig.9. All the samples exhibit typical ferroelectric loops at room temperature. It can be seen that the variation of Na/Bi stoichiometry affects the ferroelectric properties of  $(\text{Na}_{0.5}\text{Bi}_{0.5})_{1+x}\text{TiO}_3$  ceramics. P-E hysteresis loop observed for NBT0 sample without excess of Na/Bi mol% exhibits high coercive field. This may be elaborated on basis of Schottky defects resulted from Na/Bi non-stoichiometry given by following equations[45,46]:



And,



Therefore, oxygen vacancies ( $V^{\bullet\bullet}_O$ ) are created from Bi or/and Na loss which are highly mobile and interact with domain walls to hinder their movement, resulting in increased coercive field ( $E_c \sim 25.7$  kV/cm) [47].

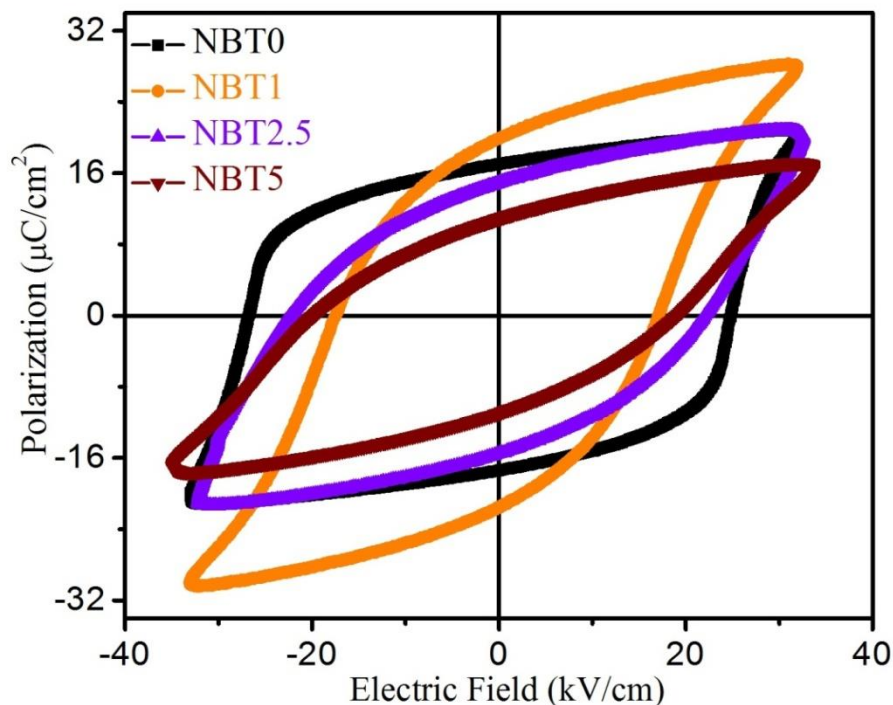


**Fig. 9.** The combined plots of room temperature polarization vs. electric field (P-E) hysteresis curves for non-stoichiometric  $(\text{Na}_{0.5}\text{Bi}_{0.5})_{1+x}\text{TiO}_3$  ceramics

A typical slim and saturated P-E hysteresis loop observed for NBT1 may arise due to the growth of stoichiometric composition without any Na/Bi loss or generation of negligible amount of oxygen vacancies in the sample. P-E hysteresis loops become more slanted for 2.5 mol% and 5mol% excess of Na/Bi which may signify that large deviation of Bi/Na stoichiometry results in weakening of long ferroelectric order in samples[45].

Fig.10. shows variation of remnant polarization ( $P_r$ ), coercive field ( $E_c$ ) and piezoelectric coefficient ( $d_{33}$ ) of  $(\text{Na}_{0.5}\text{Bi}_{0.5})_{1+x}\text{TiO}_3$  ceramic as function of concentration of Na/Bi excess addition.

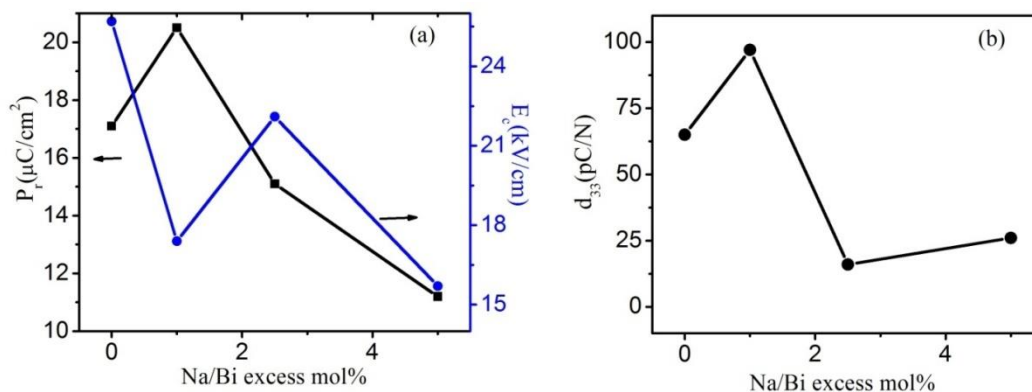


**Fig. 10.** Variation of (a) Ferroelectric parameters ( $P_r$ ,  $E_c$ ), and (b) Piezoelectric coefficient ( $d_{33}$ ) of  $(\text{Na}_{0.5}\text{Bi}_{0.5})_{1+x}\text{TiO}_3$  ceramics as a function of Na/Bi excess mol% addition

**Table 6.** Ferroelectric parameters and piezoelectric coefficient for various  $(\text{Na}_{0.5}\text{Bi}_{0.5})_{1+x}\text{TiO}_3$  ceramics

Sample	$P_{\max}$ ( $\mu\text{C}/\text{cm}^2$ )	$P_r$ ( $\mu\text{C}/\text{cm}^2$ )	$E_c$ (kV/cm)	$d_{33}$
NBT0	20.8	17.1	25.7	65
NBT1	29.2	20.5	17.4	97
NBT2.5	20.8	15.1	22.1	16
NBT5	17.1	11.2	15.7	26

It can be seen that maximum values of  $P_r \sim 20.5 \mu\text{C}/\text{cm}^2$ ,  $d_{33} \sim 97 \text{ pC}/\text{N}$  and minimum value of  $E_c \sim 17.4 \text{ kV}/\text{cm}$  is achieved for NBT1 ceramics with 1mol% of Na/Bi excess addition, whereas  $P_r$  and  $d_{33}$  values decrease with further increase of Na/Bi excess addition. The values of  $P_r$ ,  $E_c$  and  $d_{33}$  for all samples are given in Table 6. The enhancement of ferroelectric and piezoelectric properties of NBT1 may be attributed to compensation of Bi loss, compact crystal growth with uniform grains connectivity which leads to easier movement of domains and comparatively long range ferroelectric order. However, decrement of ferroelectric as well as piezoelectric properties at higher Na/Bi excess concentration i.e. at  $x = 0.05$ (NBT2.5) &  $x = 0.1$ (NBT5) may correspond to the segregation of  $\text{Na}^+$  and  $\text{Bi}^{3+}$  ions at grain boundaries which come into play due to incorporation of excess Na/Bi in crystal structure. In general, the stability of ferroelectric domains in  $\text{ABO}_3$  type perovskites depends on the coupling between  $\text{TiO}_6$  octahedra with A-site cations. The segregation of  $\text{Na}^+$  and  $\text{Bi}^{3+}$  ions hinders the coupling of  $\text{TiO}_6$  octahedra which result in reduction of ferroelectric domains stability [27, 48, 49].

In order to investigate the temperature stability of ferroelectric behavior in  $(\text{Na}_{0.5}\text{Bi}_{0.5})_{1+x}\text{TiO}_3$  ceramics, the temperature dependent P-E hysteresis loops have been measured in temperature range 30-200°C and are shown in Figs. 11 (a)-(d). The P-E hysteresis loop of NBT0 ceramic at a temperature of 30°C as in Fig 11(a) shows a typical ferroelectric shape. As the temperature is increased to 200°C, the shape of hysteresis loops appears narrow, but retains the characteristics of ferroelectric behavior. No deformation of P-E hysteresis loop is observed indicating the existence of ferroelectric character. As the temperature increases, the polarization values of NBT0 ceramics increases up to applied temperature of 200°C and coercive field decreases. The similar temperature dependent ferroelectric behavior can be noticed for NBT1, NBT2.5 and NBT5 ceramics as shown in Figs 11(b)-11(d).

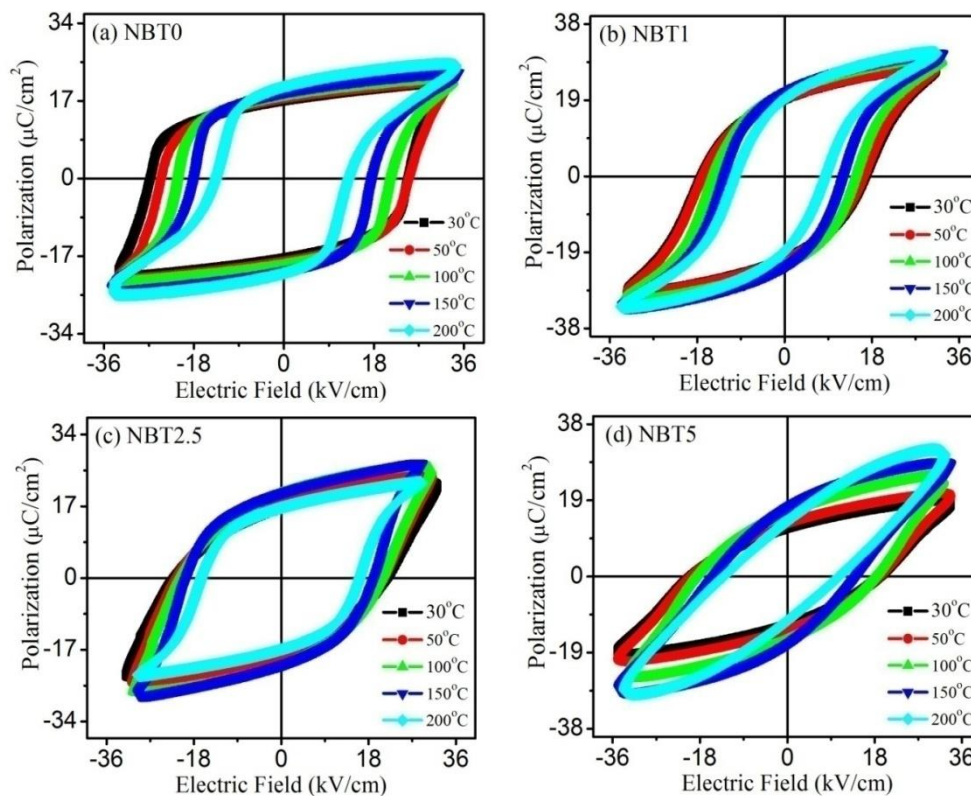


**Fig. 11.** The P-E hysteresis loops of  $(\text{Na}_{0.5}\text{Bi}_{0.5})_{1+x}\text{TiO}_3$  ceramics at various temperatures with Na/Bi excess mol% (a) 0, (b) 1, (c) 2.5 and (d) 5

The area of hysteresis loop which is a measure of energy loss is influenced by concentration of Na/Bi excess addition in NBT ceramics. The area of P-E hysteresis loop decreases with the increasing Na/Bi excess addition in NBT ceramics and the loop becomes linear at 5mol% Na/Bi excess concentration. The observation of ferroelectric hysteresis loops for all NBT ceramics over measured temperature range up to 200°C reveals the presence of ferroelectric order in these samples. The result is consistent with dielectric properties of  $(\text{Na}_{0.5}\text{Bi}_{0.5})_{1+x}\text{TiO}_3$  ceramics, where the observed depolarization temperature  $T_d$  lies well above 200°C. The decrease in coercive field ( $E_c$ ) with increase of temperature for all samples may be attributed to decrease in domain switching resistance. On the other hand remnant polarization ( $P_r$ ) values for NBT0 and NBT1 samples prolong up to the temperature 200°C with typical ferroelectric hysteresis loop shape whereas the  $P_r$  values decrease significantly for NBT2.5 and NBT5 samples at 200°C with the appearance of slightly distorted hysteresis loop.

#### IV. CONCLUSIONS

In summary, we have systematically studied the effect of Na/Bi excess mol% on structural, dielectric, ferroelectric and piezoelectric properties of  $(\text{Na}_{0.5}\text{Bi}_{0.5})_{1+x}\text{TiO}_3$  ceramics. A pure perovskite crystal structure is observed for 0 to 5 mol% excess of Na/Bi in  $(\text{Na}_{0.5}\text{Bi}_{0.5})_{1+x}\text{TiO}_3$  ceramics based on x-ray diffraction and Raman spectra analysis. Elemental analysis by EDS reveals Bi loss in NBT0, surplus alkali (Na) in NBT2.5 and NBT5 and stoichiometric composition (Bi/Na ~1) in NBT1 sample which is supported by surface morphology, relative density and DC resistivity measurements. Compositional fluctuations induced due to excess mol% of Na/Bi result in variation in dielectric as well as ferroelectric and piezoelectric properties. Complex impedance analysis is under progress for more clear understanding of electrical transport phenomenon in  $(\text{Na}_{0.5}\text{Bi}_{0.5})_{1+x}\text{TiO}_3$  ceramics. Temperature dependent PE curves for NBT0 and NBT1 represents stable ferroelectric order up to 200°C temperature which is in good agreement of depolarisation temperature ( $T_d$ ) observed during dielectric measurements. Therefore, we can conclude that adequate control of Na/Bi excess mol% in  $(\text{Na}_{0.5}\text{Bi}_{0.5})_{1+x}\text{TiO}_3$  ceramics lead to improve the structural as well as electrical properties.

**ACKNOWLEDGEMENT**

One of the authors (K. Parmar) is thankful to UGC, New Delhi for providing financial assistance under grants No: F.11-83/2008 (BSR). The help provided by Prof. A.K. Saini, PU Chandigarh for Raman Spectroscopy measurement is acknowledged.

**REFERENCES**

- [1] Y. Saito, H. Takao, T. Tani, T. Nonoyama, K. Takatori, T. Homma, T. Nagaya, M. Nakamura, Lead-free piezoceramics, *Nature*, 432 (2004) 84-87.  
<http://dx.doi.org/10.1038/nature03028>
- [2] Y. Li, W. Chen, Q. Xu, J. Zhou, Y. Wang, H. Sun, Piezoelectric and dielectric properties of CeO 2-doped Bi 0.5 Na 0.44 K 0.06 TiO 3 lead-free ceramics, *Ceramics international*, 33 (2007) 95-99.  
<http://dx.doi.org/10.1016/j.ceramint.2005.08.001>
- [3] J. Rödel, W. Jo, K.T. Seifert, E.M. Anton, T. Granzow, D. Damjanovic, Perspective on the Development of Lead-free Piezoceramics, *Journal of the American Ceramic Society*, 92 (2009) 1153-1177.  
<http://dx.doi.org/10.1111/j.1551-2916.2009.03061.x>
- [4] H. Gu, A. Kuang, S. Wang, D. Bao, L. Wang, J. Liu, X. Li, Synthesis and ferroelectric properties of c-axis oriented Bi<sub>4</sub>Ti<sub>3</sub>O<sub>12</sub> thin films by sol-gel process on platinum coated silicon, *Applied physics letters*, 68 (1996) 1209-1210.  
<http://dx.doi.org/10.1063/1.115971>
- [5] S.T. Zhang, A.B. Kounga, E. Aulbach, T. Granzow, W. Jo, H.-J. Kleebe, J. Rödel, Lead-free piezoceramics with giant strain in the system Bi<sub>0.5</sub>Na<sub>0.5</sub>TiO<sub>3</sub>-BaTiO<sub>3</sub>-K<sub>0.5</sub>Na<sub>0.5</sub>NbO<sub>3</sub>. I. Structure and room temperature properties, *Journal of Applied Physics*, 103 (2008) 034107.  
<http://dx.doi.org/10.1063/1.2838472>
- [6] A.B. Kounga, S.-T. Zhang, W. Jo, T. Granzow, J. Rödel, Morphotropic phase boundary in „1- x... Bi 0.5 Na 0.5 TiO 3-x K 0.5 Na 0.5 NbO 3 lead-free piezoceramics, *Applied Physics Letters*, 92 (2008) 222902.  
<http://dx.doi.org/10.1063/1.2938064>
- [7] Y. Guo, M. Gu, H. Luo, Y. Liu, R.L. Withers, Composition-induced antiferroelectric phase and giant strain in lead-free (Na<sub>y</sub>, Bi<sub>z</sub>)Ti<sub>1-x</sub>O<sub>3</sub>(1-x)-xBaTiO<sub>3</sub> ceramics, *Physical Review B*, 83 (2011) 054118.  
<http://dx.doi.org/10.1103/PhysRevB.83.054118>
- [8] V.V. Shvartsman, D.C. Lupascu, Lead-Free Relaxor Ferroelectrics, *Journal of the American Ceramic Society*, 95 (2012) 1-26.  
<http://dx.doi.org/10.1111/j.1551-2916.2011.04952.x>
- [9] T. Takenaka, K.I. Maruyama, K. Sakata, (Bi<sub>1/2</sub>Na<sub>1/2</sub>)TiO<sub>3</sub>-BaTiO<sub>3</sub> system for lead-free piezoelectric ceramics, *Japanese Journal of Applied Physics*, 30 (1991) 2236.  
<http://dx.doi.org/10.1143/JJAP.30.2236>
- [10] V. Isupov, Ferroelectric Na<sub>0.5</sub>Bi<sub>0.5</sub>TiO<sub>3</sub> and K<sub>0.5</sub>Bi<sub>0.5</sub>TiO<sub>3</sub> perovskites and their solid solutions, *Ferroelectrics*, 315 (2005) 123-147.  
<http://dx.doi.org/10.1080/001501990910276>
- [11] K. Sakata, Y. Masuda, Ferroelectric and antiferroelectric properties of (Na 0.5 Bi 0.5) TiO<sub>3</sub>-SrTiO<sub>3</sub> solid solution ceramics, *Ferroelectrics*, 7 (1974) 347-349.  
<http://dx.doi.org/10.1080/00150197408238042>
- [12] G. Jones, P. Thomas, Investigation of the structure and phase transitions in the novel A-site substituted distorted perovskite compound Na<sub>0.5</sub>Bi<sub>0.5</sub>TiO<sub>3</sub>, *Acta Crystallographica Section B: Structural Science*, 58 (2002) 168-178.  
<http://dx.doi.org/10.1107/S0108768101020845>
- [13] M. Zannen, H. Khemakhem, A. Kabadou, M. Es-Souni, Structural, Raman and electrical studies of 2at.% Dy-doped NBT, *Journal of Alloys and Compounds*, 555 (2013) 56-61.  
<http://dx.doi.org/10.1016/j.jallcom.2012.12.002>
- [14] V. Dorcet, G. Trolliard, P. Boullay, Reinvestigation of phase transitions in Na<sub>0.5</sub>Bi<sub>0.5</sub>TiO<sub>3</sub> by TEM. Part I: First order rhombohedral to orthorhombic phase transition, *Chemistry of Materials*, 20 (2008) 5061-5073.  
<http://dx.doi.org/10.1021/cm8004634>
- [15] C. Ma, X. Tan, In situ Transmission Electron Microscopy Study on the Phase Transitions in Lead-Free (1-x)(Bi<sub>1/2</sub>Na<sub>1/2</sub>)TiO<sub>3</sub>-xBaTiO<sub>3</sub> Ceramics, *Journal of the American Ceramic Society*, 94 (2011) 4040-4044.  
<http://dx.doi.org/10.1111/j.1551-2916.2011.04670.x>
- [16] B.N. Rao, R. Datta, S.S. Chandrashekar, D.K. Mishra, V. Sathe, A. Senyshyn, R. Ranjan, Local structural disorder and its influence on the average global structure and polar properties in Na 0.5 Bi 0.5 TiO 3, *Physical Review B*, 88 (2013) 224103.  
<http://dx.doi.org/10.1103/PhysRevB.88.224103>

- [17] S. Gorfman, P.A. Thomas, Evidence for a non-rhombohedral average structure in the lead-free piezoelectric material  $\text{Na}_0.5\text{Bi}_0.5\text{TiO}_3$ , *Journal of Applied Crystallography*, 43 (2010) 1409-1414.  
<http://dx.doi.org/10.1107/S002188981003342X>
- [18] E. Aksel, J.S. Forrester, J.L. Jones, P.A. Thomas, K. Page, M.R. Suchomel, Monoclinic crystal structure of polycrystalline  $\text{Na}_0.5\text{Bi}_0.5\text{TiO}_3$ , *Applied Physics Letters*, 98 (2011) 152901.  
<http://dx.doi.org/10.1063/1.3573826>
- [19] G. Viola, H. Ning, M. Reece, R. Wilson, T. Correia, P. Weaver, M. Cain, H. Yan, Reversibility in electric field-induced transitions and energy storage properties of bismuth-based perovskite ceramics, *Journal of Physics D: Applied Physics*, 45 (2012) 355302.  
<http://dx.doi.org/10.1088/0022-3727/45/35/355302>
- [20] C. Xu, D. Lin, K. Kwok, Structure, electrical properties and depolarization temperature of  $(\text{Bi}_{0.5}\text{Na}_{0.5})\text{TiO}_3$  lead-free piezoelectric ceramics, *Solid State Sciences*, 10 (2008) 934-940.  
<http://dx.doi.org/10.1016/j.solidstatesciences.2007.11.003>
- [21] H. Nagata, T. Shinya, Y. Hiruma, T. Takenaka, I. Sakaguchi, H. Haneda, Piezoelectric Properties of Bismuth Sodium Titanate Ceramics, *Developments in Dielectric Materials and Electronic Devices*, Volume 167(2006) 213-221.  
<http://dx.doi.org/10.1002/9781118408186.ch20>
- [22] R. Zuo, S. Su, Y. Wu, J. Fu, M. Wang, L. Li, Influence of A-site nonstoichiometry on sintering, microstructure and electrical properties of  $(\text{Bi}_{0.5}\text{Na}_{0.5})\text{TiO}_3$  ceramics, *Materials Chemistry and Physics*, 110 (2008) 311-315.  
<http://dx.doi.org/10.1016/j.matchemphys.2008.02.007>
- [23] Y. Sung, J. Kim, J. Cho, T. Song, M. Kim, T. Park, Effects of Bi nonstoichiometry in  $(\text{Bi}_{0.5+x}\text{Na})\text{TiO}_3$  ceramics, *Applied Physics Letters*, 98 (2011) 012902.  
<http://dx.doi.org/10.1063/1.3525370>
- [24] X. Chen, H. Ma, W. Pan, M. Pang, P. Liu, J. Zhou, Microstructure, dielectric and ferroelectric properties of  $(\text{Na}_x\text{Bi}_{0.5-x})_{0.94}\text{Ba}_{0.06}\text{TiO}_3$  lead-free ferroelectric ceramics: Effect of Na nonstoichiometry, *Materials Chemistry and Physics*, 132 (2012) 368-374.  
<http://dx.doi.org/10.1016/j.matchemphys.2011.11.039>
- [25] A. Li, J. Wu, S. Qiao, W. Wu, B. Wu, D. Xiao, J. Zhu, Microstructure and electrical properties of  $(\text{Bi}_{0.5-x}\text{Na}_x)_{0.94}\text{Ba}_{0.06}\text{TiO}_3$  ceramics with bismuth nonstoichiometry, *physica status solidi (a)*, 209 (2012) 1213-1218.  
<http://dx.doi.org/10.1002/pssa.201127744>
- [26] Y. Guo, H. Fan, C. Long, J. Shi, L. Yang, S. Lei, Electromechanical and electrical properties of  $\text{Bi}_{0.5}\text{Na}_{0.5}\text{Ti}_{1-x}\text{Mn}_x\text{O}_{3-\delta}$  ceramics with high remnant polarization, *Journal of Alloys and Compounds*, 610 (2014) 189-195.  
<http://dx.doi.org/10.1016/j.jallcom.2014.04.038>
- [27] Y. Sung, J. Kim, J. Cho, T. Song, M. Kim, H. Chong, T. Park, D. Do, S. Kim, Effects of Na nonstoichiometry in  $(\text{Bi}_{0.5-x}\text{Na}_x)\text{TiO}_3$  ceramics, *Applied Physics Letters*, 96 (2010) 022901.  
<http://dx.doi.org/10.1063/1.3275704>
- [28] K. Parmar, N. Negi, Influence of Na/Bi excess on structural, dielectric and multiferroic properties of lead free  $(\text{Na}_{0.5}\text{Bi}_{0.5})_{0.99}\text{La}_{0.01}\text{Ti}_{0.988}\text{Fe}_{0.012}\text{O}_3$  ceramic, *Journal of Alloys and Compounds*, 618 (2015) 781-787.  
<http://dx.doi.org/10.1016/j.jallcom.2014.07.138>
- [29] Y. Hiruma, H. Nagata, T. Takenaka, Thermal depoling process and piezoelectric properties of bismuth sodium titanate ceramics, *Journal of applied physics*, 105 (2009) 084112-084112.  
<http://dx.doi.org/10.1063/1.3115409>
- [30] M. Spreitzer, M. Valant, D. Suvorov, Sodium deficiency in  $\text{Na}_{0.5}\text{Bi}_{0.5}\text{TiO}_3$ , *Journal of Materials Chemistry*, 17 (2007) 185-192.  
<http://dx.doi.org/10.1039/B609606A>
- [31] M. Li, H. Zhang, S.N. Cook, L. Li, J.A. Kilner, I.M. Reaney, D.C. Sinclair, Dramatic influence of A-site nonstoichiometry on the electrical conductivity and conduction mechanisms in the perovskite oxide  $\text{Na}_{0.5}\text{Bi}_{0.5}\text{TiO}_3$ , *Chemistry of Materials*, 27 (2015) 629-634.  
<http://dx.doi.org/10.1021/cm504475k>
- [32] J. Petzelt, S. Kamba, J. Fabry, D. Noujni, V. Porokhonsky, A. Pashkin, I. Franke, K. Roleder, J. Suchanicz, R. Klein, Infrared, Raman and high-frequency dielectric spectroscopy and the phase transitions in  $\text{Na}_{1/2}\text{Bi}_{1/2}\text{TiO}_3$ , *Journal of Physics: Condensed Matter*, 16 (2004) 2719.  
<http://dx.doi.org/10.1088/0953-8984/16/15/022>
- [33] J. Anthoniappen, C.H. Lin, C. Tu, P.Y. Chen, C.S. Chen, S.J. Chiu, H.Y. Lee, S.F. Wang, C.M. Hung, Enhanced Piezoelectric and Dielectric Responses in 92.5%  $(\text{Bi}_{0.5}\text{Na}_{0.5})\text{TiO}_3$ -7.5%  $\text{BaTiO}_3$  Ceramics, *Journal of the American Ceramic Society*, 97 (2014) 1890-1894.

<http://dx.doi.org/10.1111/jace.12864>

[34] A.P.B. Selvadurai, V. Pazhivelu, B. Vasanth, C. Jagadeeshwaran, R. Murugaraj, Investigation of structural and optical spectroscopy of 5% Pr doped (Bi<sub>0.5</sub>Na<sub>0.5</sub>)TiO<sub>3</sub> ferroelectric ceramics: site depended study, Journal of Materials Science: Materials in Electronics, 26 (2015) 7655-7665.

<http://dx.doi.org/10.1007/s10854-015-3405-5>

[35] K. Thangavelu, R. Ramadurai, S. Asthana, Evidence for the suppression of intermediate anti-ferroelectric ordering and observation of hardening mechanism in Na<sub>1/2</sub>Bi<sub>1/2</sub>TiO<sub>3</sub> ceramics through cobalt substitution, AIP Advances, 4 (2014) 017111.

<http://dx.doi.org/10.1063/1.4862169>

[36] K. Mishra, V. Sivasubramanian, R. Sarguna, T. Ravindran, A. Arora, Raman scattering from La-substituted BiFeO<sub>3</sub>-PbTiO<sub>3</sub>, Journal of Solid State Chemistry, 184 (2011) 2381-2386.

<http://dx.doi.org/10.1016/j.jssc.2011.07.014>

[37] M.K. Niranjan, T. Karthik, S. Asthana, J. Pan, U.V. Waghmare, Theoretical and experimental investigation of Raman modes, ferroelectric and dielectric properties of relaxor Na<sub>0.5</sub>Bi<sub>0.5</sub>TiO<sub>3</sub>, Journal of Applied Physics, 113 (2013) 194106.

<http://dx.doi.org/10.1063/1.4804940>

[38] A. O'Brien, D.I. Woodward, K. Sardar, R.I. Walton, P.A. Thomas, Inference of oxygen vacancies in hydrothermal Na<sub>0.5</sub>Bi<sub>0.5</sub>TiO<sub>3</sub>, Applied Physics Letters, 101 (2012) 142902.

<http://dx.doi.org/10.1063/1.4755882>

[39] M. Zhu, H. Hu, N. Lei, Y. Hou, H. Yan, Dependence of depolarization temperature on cation vacancies and lattice distortion for lead-free 74 (Bi<sub>1/2</sub>Na<sub>1/2</sub>)TiO<sub>3</sub>-20.8 (Bi<sub>1/2</sub>K<sub>1/2</sub>)TiO<sub>3</sub>-5.2 BaTiO<sub>3</sub> ferroelectric ceramics, Applied Physics Letters, 94 (2009) 182901.

<http://dx.doi.org/10.1063/1.3130736>

[40] X. Chen, Y. Liao, H. Wang, L. Mao, D. Xiao, J. Zhu, Q. Chen, Phase structure and electric properties of Bi<sub>0.5</sub>(Na<sub>0.825</sub>K<sub>0.175</sub>)<sub>0.5</sub>TiO<sub>3</sub> ceramics prepared by a sol-gel method, Journal of Alloys and Compounds, 493 (2010) 368-371.

<http://dx.doi.org/10.1016/j.jallcom.2009.12.104>

[41] E.M. Anton, W. Jo, D. Damjanovic, J. Rödel, Determination of depolarization temperature of (Bi<sub>1/2</sub>Na<sub>1/2</sub>)TiO<sub>3</sub>-based lead-free piezoceramics, Journal of Applied Physics, 110 (2011) 094108.

<http://dx.doi.org/10.1063/1.3660253>

[42] Z. Mankang, H. Hancheng, L. Na, H. Yudong, Y. Hui, Dependence of depolarization temperature on cation vacancies and lattice distortion for lead-free 74 (Bi<sub>1/2</sub>Na<sub>1/2</sub>)TiO<sub>3</sub>-20.8 (Bi<sub>1/2</sub>K<sub>1/2</sub>)TiO<sub>3</sub>-5.2 BaTiO<sub>3</sub> ferroelectric ceramics, Applied Physics Letters, 94 (2009).

<http://dx.doi.org/10.1063/1.3130736>

[43] S.S. Sundari, B. Kumar, R. Dhanasekaran, Synthesis, dielectric and relaxation behavior of lead free NBT-BT ceramics, Ceramics International, 39 (2013) 555-561.

<http://dx.doi.org/10.1016/j.ceramint.2012.06.063>

[44] K. Uchino, S. Nomura, Critical exponents of the dielectric constants in diffused-phase-transition crystals, Ferroelectrics, 44 (1982) 55-61.

<http://dx.doi.org/10.1080/00150198208260644>

[45] H. Zhang, C. Chen, X. Zhao, H. Deng, L. Li, D. Lin, X. Li, B. Ren, H. Luo, J. Yan, Enhanced ferroelectric properties and thermal stability of nonstoichiometric 0.92 (Na<sub>0.5</sub>Bi<sub>0.5</sub>)TiO<sub>3</sub>-0.08 (K<sub>0.5</sub>Bi<sub>0.5</sub>)TiO<sub>3</sub> single crystals, Applied Physics Letters, 103 (2013) 212906.

<http://dx.doi.org/10.1063/1.4833401>

[46] D.M. Smyth, The defect chemistry of metal oxides, The Defect Chemistry of Metal Oxides, by DM Smyth, pp. 304. Foreword by DM Smyth. Oxford University Press, Jun 2000. ISBN-10: 0195110145. ISBN-13: 9780195110142, 1 (2000).

[47] K. Yanai, Y. Kitanaka, Y. Noguchi, M. Miyayama, C. Moriyoshi, Y. Kuroiwa, K. Kurushima, S. Mori, Enhanced polarization switching in ferroelectric Bi<sub>0.5</sub>Na<sub>0.5</sub>TiO<sub>3</sub> single crystals by defect control, physica status solidi (a), 210 (2013) 791-795.

<http://dx.doi.org/10.1002/pssa.201228442>

[48] Q. Xu, D.-P. Huang, M. Chen, W. Chen, H.-X. Liu, B.-H. Kim, Effect of bismuth excess on ferroelectric and piezoelectric properties of a (Na<sub>0.5</sub>Bi<sub>0.5</sub>)TiO<sub>3</sub>-BaTiO<sub>3</sub> composition near the morphotropic phase boundary, Journal of Alloys and Compounds, 471 (2009) 310-316.

<http://dx.doi.org/10.1016/j.jallcom.2008.03.078>

[49] X. Dai, A. DiGiovanni, D. Viehland, Dielectric properties of tetragonal lanthanum modified lead zirconate titanate ceramics, Journal of applied physics, 74 (1993) 3399-3405.

<http://dx.doi.org/10.1063/1.354567>

## AUTHORS BIOGRAPHY

**Kusum Parmar** has received her M.Sc., M.Phil and Ph.D degree in Physics from Himachal Pradesh University, Shimla. She has attended 12 international/national conferences and workshops. Her area of research interest includes Ferroelectric material, multiferroics and ferrite/ferroelectric composite materials.



**N. S. Negi** joined the Himachal Pradesh University, Shimla in October 1997. He received his PhD degree from the Himachal Pradesh University Shimla. He has extensive experience in deposition of ferroelectric & ferrite thin films. He currently works on ferroelectric & multiferroic thin films, high k materials, diluted magnetic semiconductors & pyrophoric materials. He has published over 40 papers in international journals. Currently he is a Professor and Head, Department of Physics.

